Wyznaczanie mas dla nuklidów dalekich od ścieżki stabilności

Zygmunt Patyk

Narodowe Centrum Badań Jądrowych, Warszawa

Plan seminarium

- Masy jąder atomowych mierzone są w GSI-Darmstadt w pierścieniu akumulacyjnym (ESR) przy użyciu dwóch technik – metody Schottky'ego (SMS) oraz tzw. metody czasu przelotu (IMS).
- Tymi dwiema metodami wyznaczono masy dla ponad 300 jąder atomowych.
- W pierwszej metodzie błąd pomiaru był mniejszy niż 30 keV, w drugiej wahał się w przedziale 100-200 keV.
- Ostatnio intensywnie rozwijana jest metoda pomiaru mas, polegająca na wielokrotnym odbijaniu jonu w kontrolowanym potencjale elektromagnetycznym (Multi-Reflection MR-TOF-MS).
- Omówię tę metodę wraz z podaniem jej błędu.
- Omówię też jakość współczesnych modeli teoretycznych w opisie masy jądra atomowego.

Mass Measurements of Exotic Nuclides at GSI

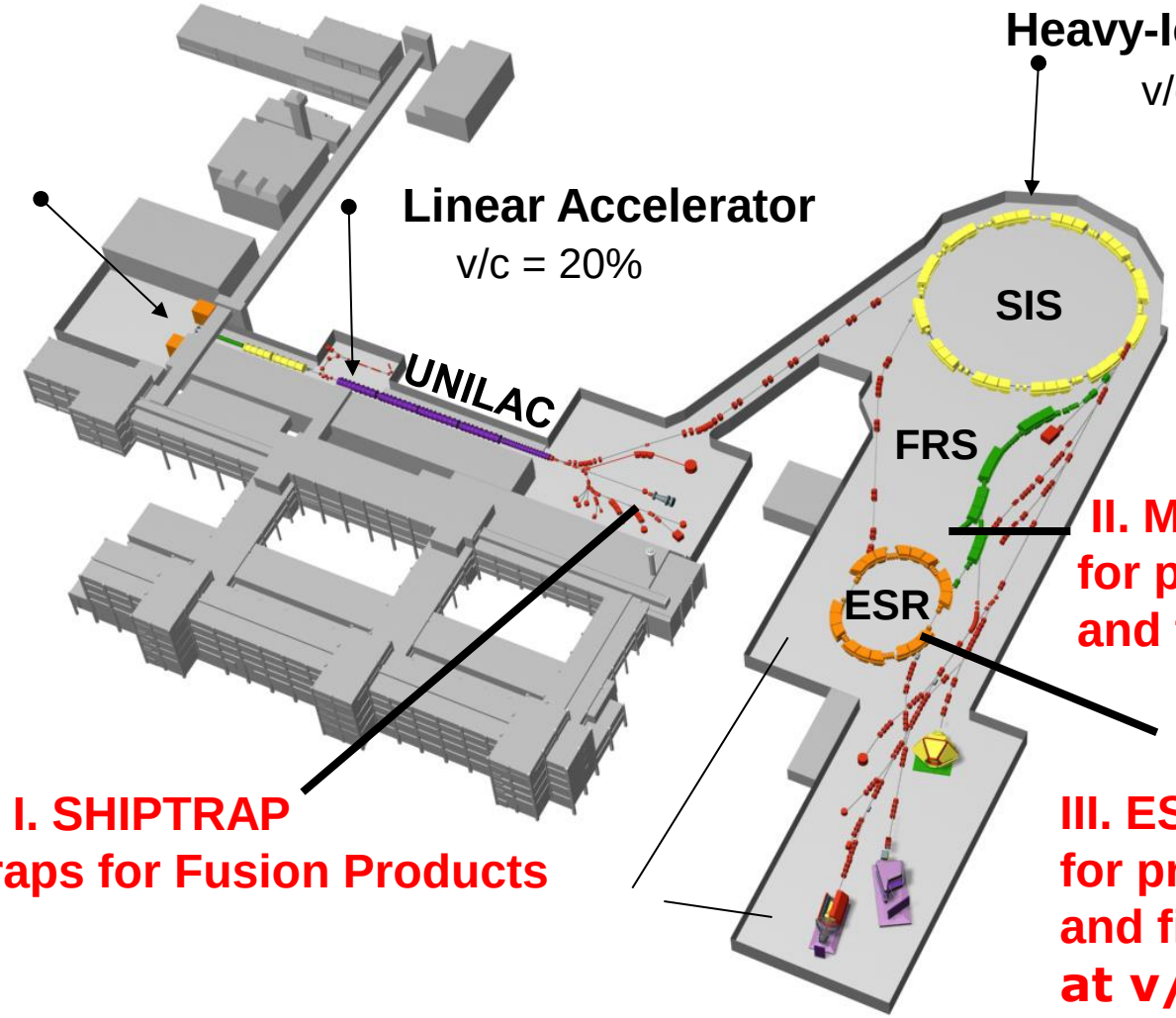

II. MR-ToF-MS
for projectile fragments
and fission products

I. SHIPTRAP
Penning-Traps for Fusion Products

III. ESR [SMS,IMS]
for projectile fragments
and fission products
at v/c=70%

Precision Mass Measurements in the ESR

SMS

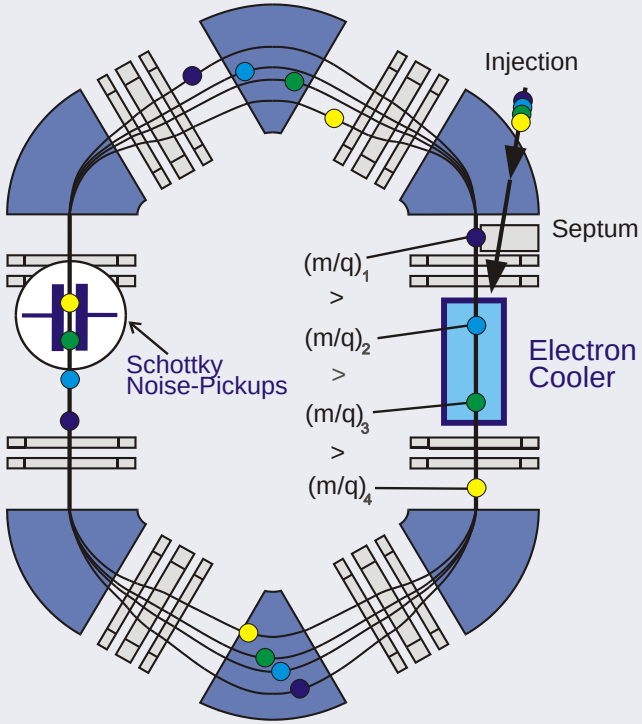

Cooled Fragments

IMS

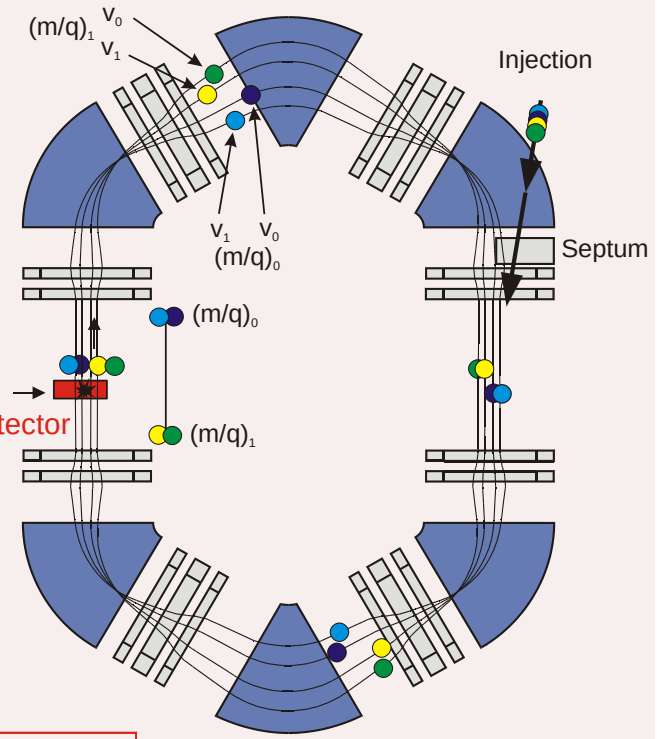

Hot Fragments

$$\frac{\Delta v}{v} \to 0 \qquad \gamma_t \to \gamma$$

$$\frac{\Delta f}{f} = -\frac{1}{\gamma_t^2}\frac{\Delta(m/q)}{m/q} + \frac{\Delta v}{v}\left(1-\frac{\gamma^2}{\gamma_t^2}\right)$$

Zasada działania spektrometrów masowych

Metody Schottky i IMS

$M*v*v/R=q*v*B \rightarrow M/q=(B/2\pi)*T$

Bardziej ogólnie: M/q=f(T), gdzie f(T) to pewna (jednoznaczna) funkcja.

Metoda MR-TOF-MS

$M*v*v/2=q*dV \rightarrow M/q=2*(dV/L/L)*T*T$

V=T/L

Wyznaczanie mas w metodzie SMS i IMS

The experimental part L_{exp} has the form

$$L_{exp} = \prod_{j,\mu} f\left(M_j/q_j - P_n^{\mu}(t_j), \delta_j^{\mu}\right), \tag{6}$$

where the product runs over all revolution times t_j belonging to the projected spectrum labelled by the index μ.

$$f(x-\mu,\sigma) = \frac{1}{\sqrt{2\pi}\sigma}\exp\left(-\frac{(x-\mu)^2}{2\sigma^2}\right),$$

with μ as the mean value and σ as the width of the distribution.

The calibration part L_c is defined as

$$L_c = \prod_i f\left(M_i^b - \widetilde{M_i^b}, \delta\widetilde{M_i^b}\right)$$

and contains the nuclear masses of bare ions M_i^b as free parameters.

The statistical error has been estimated for each nuclide from the square root of the diagonal element of the inverse correlation matrix

$$\sigma_i = \sqrt{\left(W^{-1}\right)_{i,i}}. \tag{9}$$

Elements of the correlation matrix W are given by the expression (for details see Eqs. (25)–(26) published in the paper [27]):

$$W_{i,j} = -\frac{\partial^2 \ln L}{\partial M_i^b \partial M_j^b}. \tag{10}$$

Velocity Profile of the Electron Beam Influence on the Mass Measurements

L. Chen et al., Nucl. Phys. A 882 (2012) 71.

$$\frac{f_i - f_j}{f_i} = -\alpha_p\left[\frac{(m/q)_i - (m/q)_j}{(m/q)_i}\right] + \left(1 - \frac{\gamma^2}{\gamma_t^2}\right)\left(\frac{v_i - v_j}{v_i}\right)$$

$$\Delta E(r) = n_e \pi r_e m_e c^2 r^2$$

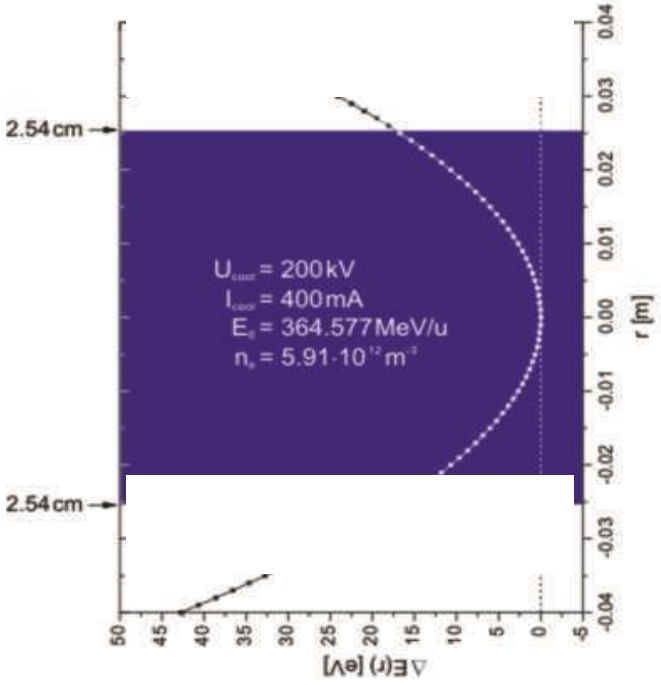

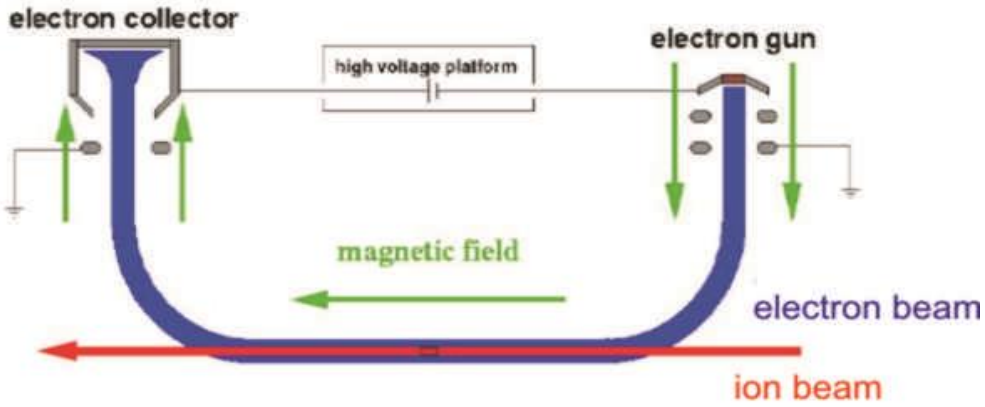

$$R_{16} \approx 1 cm/\%$$

$$r = R_{16} \cdot \frac{\Delta B\rho}{B\rho}$$

H. Poth, Phys. Rep. 196 (1990) 135.
M. Steck, Beam Cooling, Talk at the CERN Accelerator School Darmstadt, 28.09.2009-09.10.2009.
C. Brandau, Dissertation, Justus-Liebig-Universität Gießen, 2000.

$$\sum_i \frac{(M_i^b - M_{i,syst}^b)^2}{(\delta M_{i,syst}^b)^2 + (\sigma_i^{stat})^2 + (\sigma^{syst})^2} = N_n$$

Systematic Error
$\sigma^{syst} \approx 10$ keV

Correlated mass shift observed in the SMS method

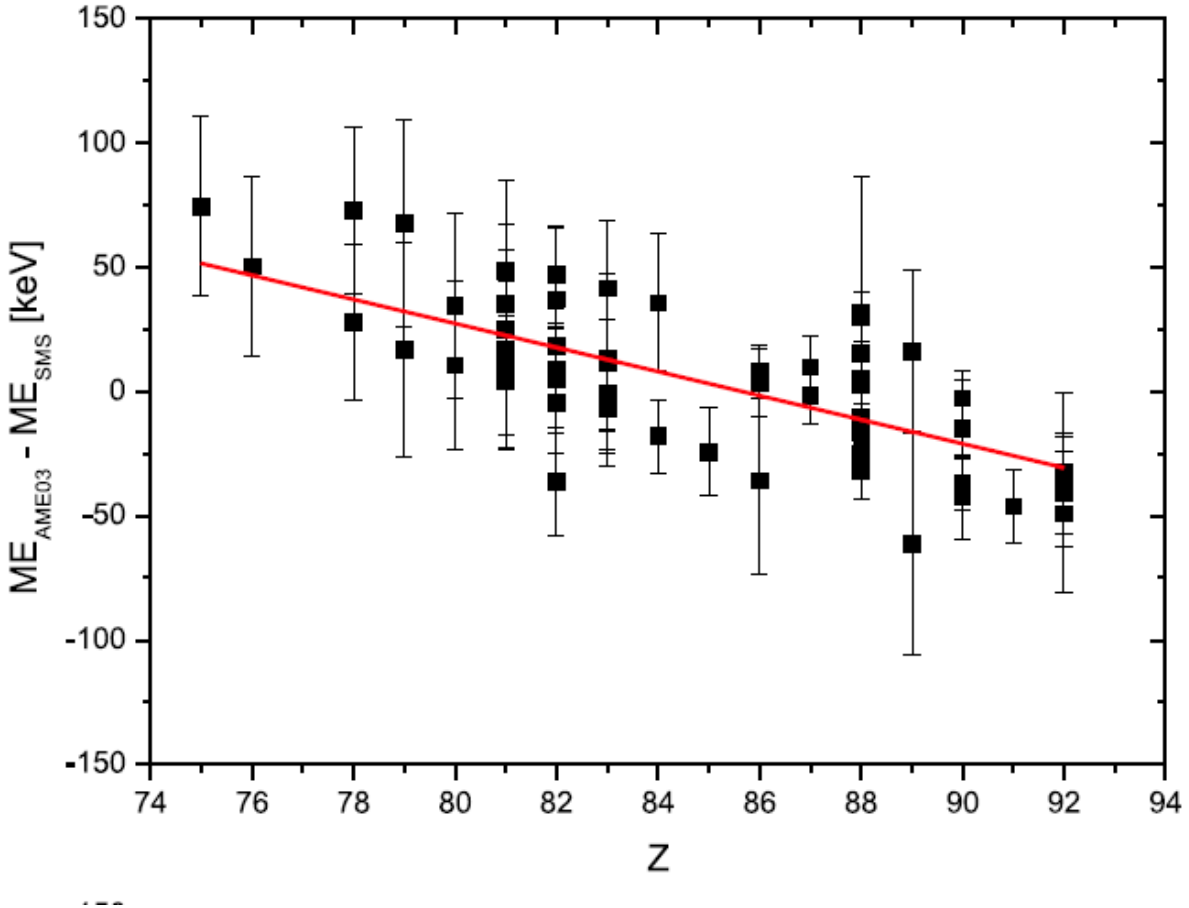

Fig. 4. Upper panel: Observation of systematic deviations of reference masses to their values given in AME03 [30] found after the first evaluation with the correlation matrix method. Lower panel: Calculated deviations from the reference mass

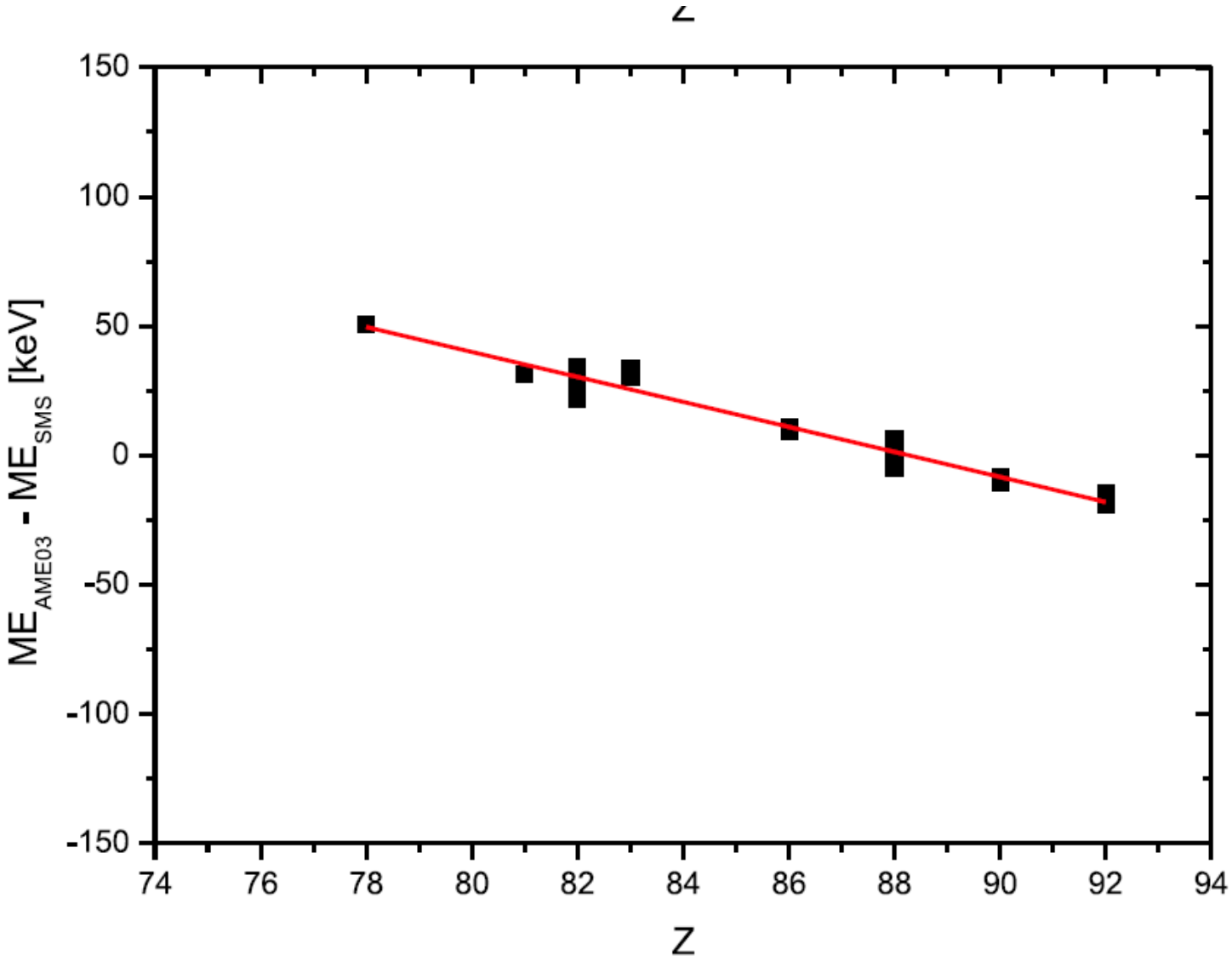

after the first evaluation with the correlation matrix method. Lower panel: Calculated deviations from the reference mass values in Atomic Mass Evaluation [30] taking into account the radial profile of the longitudinal velocity of the cooler electrons, see text. One can reproduce the observed dependence presented in the upper panel by calculations including an ion-optical dispersion coefficient of 1.06 cm/% and an offset from the ion-optical axis of 2.4 mm.

List of nuclei with mass excess (*ME*) values measured for the first time in the present experiment [10]. The σ_{ME} values are the corresponding errors. Newly discovered isotopes are marked in bold.

Element	*Z*	*N*	*A*	*ME* (keV)	σ_{ME} (keV)
Pt	78	124	202	−22692	25
Tl	**81**	**132**	**213**	**1784**	**27**
Bi	83	134	217	8730	18
	83	135	218	13216	27
Po	84	135	219	12681	16
	84	136	220	15263	18
	84	**137**	**221**	**19774**	**20**
	84	**138**	**222**	**22486**	**40**
At	85	136	221	16783	14
	85	137	222	20953	16
	85	138	223	23428	14
	85	**139**	**224**	**27711**	**22**
Rn	86	137	223	20381	12
	86	138	224	22453	13
	86	139	225	26526	13
	86	140	226	28753	14
	86	141	227	32905	23
	86	142	228	35234	29
Fr	87	141	228	33367	15
	87	143	230	39515	19
	87	144	231	42064	25
Ra	88	143	231	38212	14
	88	144	232	40496	14
	88	145	233	44322	16
	88	146	234	46893	31
Ac	89	144	233	41308	13
	89	145	234	44841	14
	89	146	235	47357	14
	89	**147**	**236**	**51221**	**38**
Th	90	146	236	46255	14
	90	147	237	49955	16

L. Chen et al. „New results on mass measurements of stored neutron-rich nuclides in the element range from Pt to U with the FRS-ESR facility at 360–400 MeV/u" Nuclear Physics A 882 (2012) 71–89

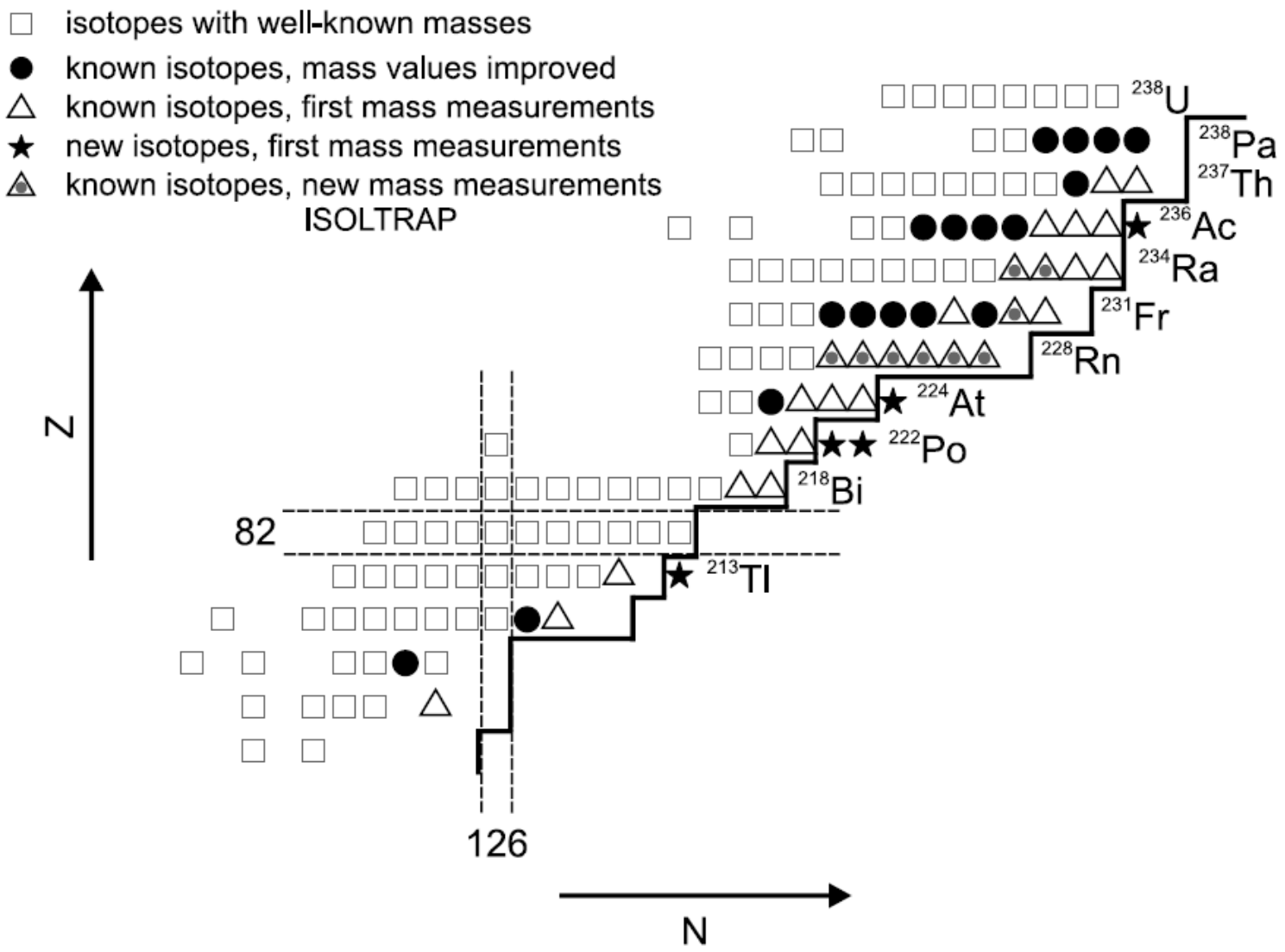
isotopes with well-known masses
known isotopes, mass values improved
known isotopes, first mass measurements
new isotopes, first mass measurements
known isotopes, new mass measurements
ISOLTRAP
238U
238Pa
237Th
236Ac
234Ra
231Fr
228Rn
224At
222Po
218Bi
213Tl
82
126
Z
N

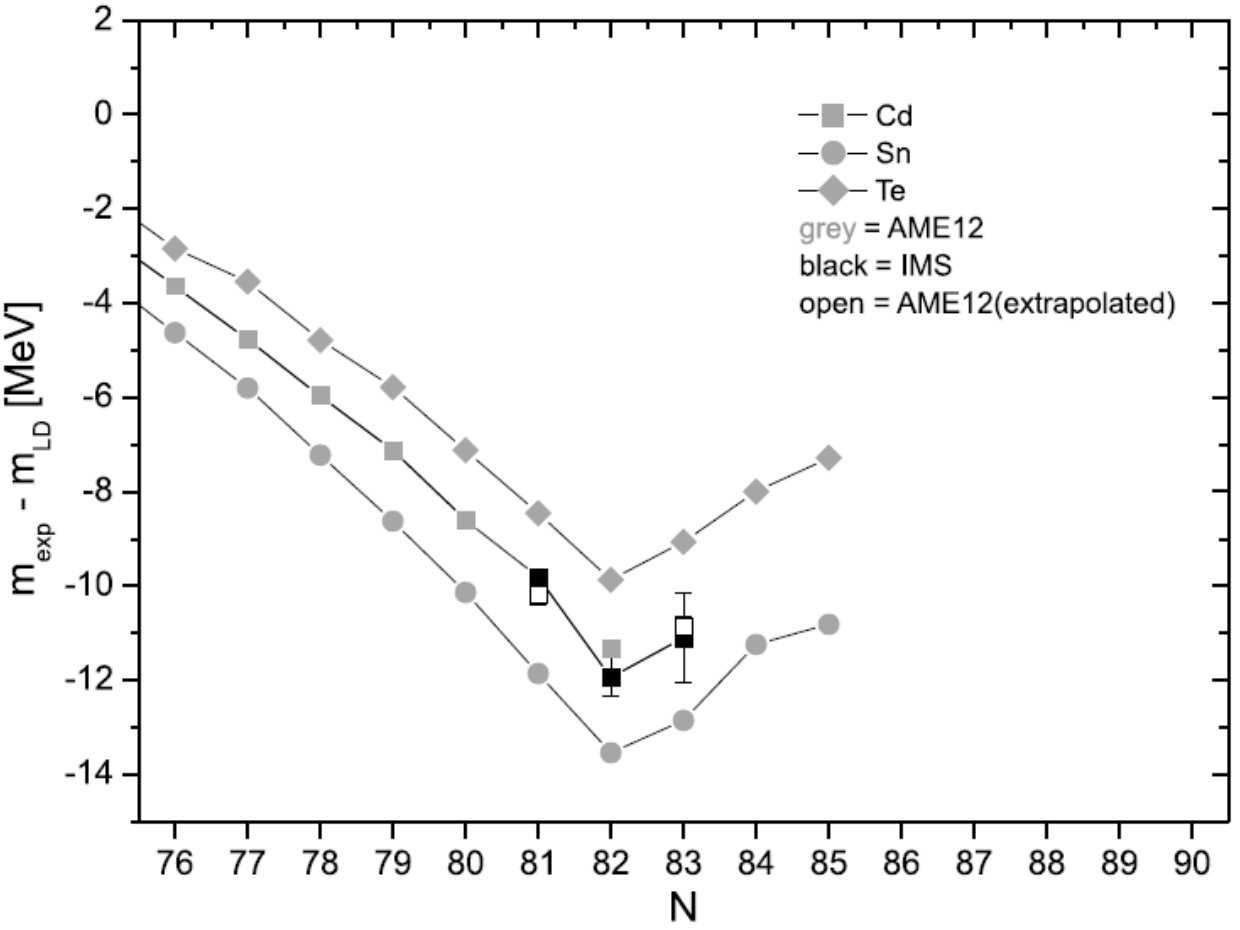

Fig. 2. Difference between the measured mass values and the smooth Weizsäcker formula given by Eq. (3) for the elements tellurium, tin and cadmium. The parameters used in the formula are presented in the text. The data clearly show the extra binding energy due to the contribution of the shell structure for all three elements in this mass region of $N = 82$.

Isochronous Mass Spectrometry IMS

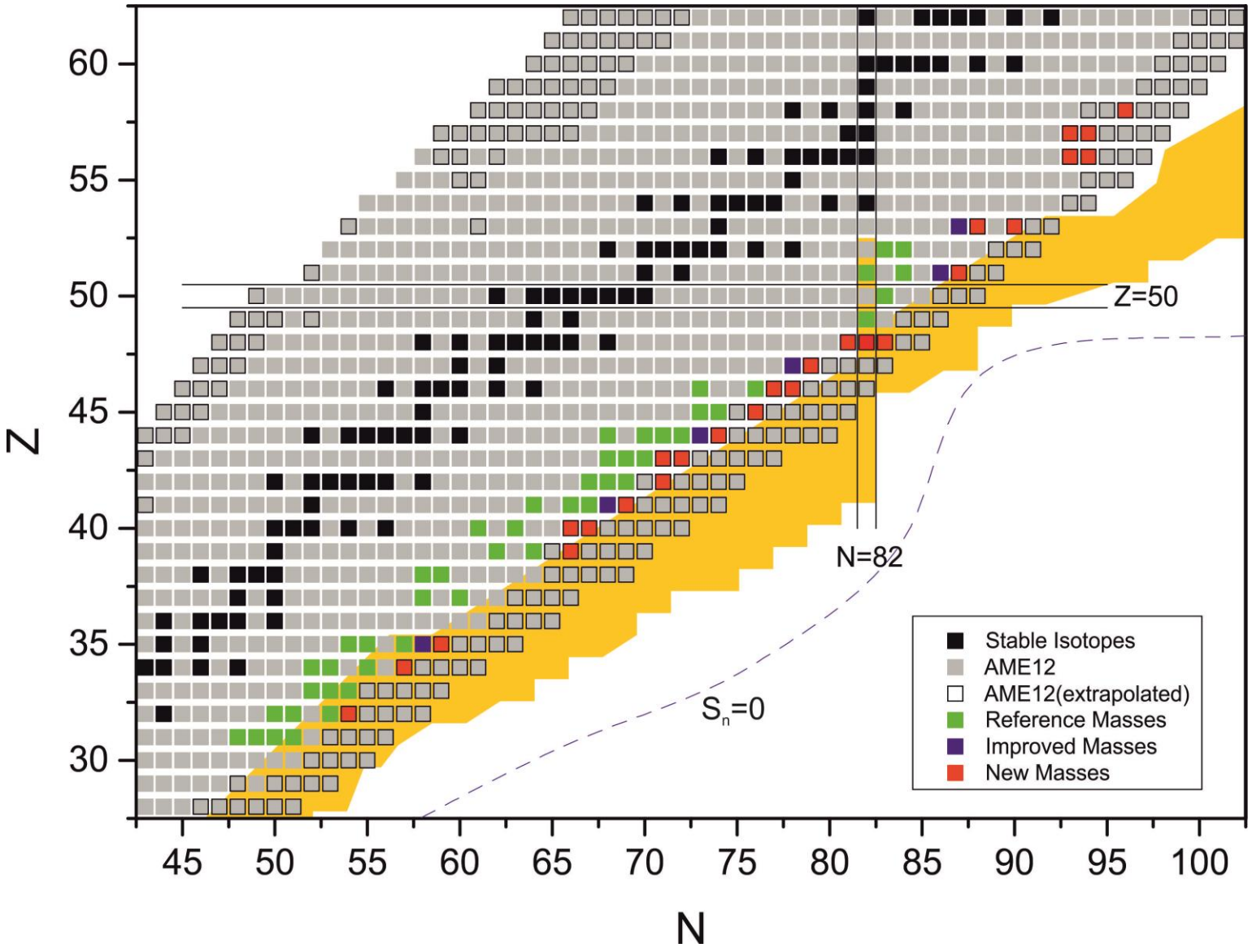

R.Knoebel and M. Diwisch

Mass Surface measured with the SMS + IMS

Masses of more than 1000 Nuclides were measured

Mass accuracy: $1.5 \cdot 10^{-7}$

Mass resolving power: $2 \cdot 10^{6}$

Results: 320 new masses

In addition more than 300 improved mass values

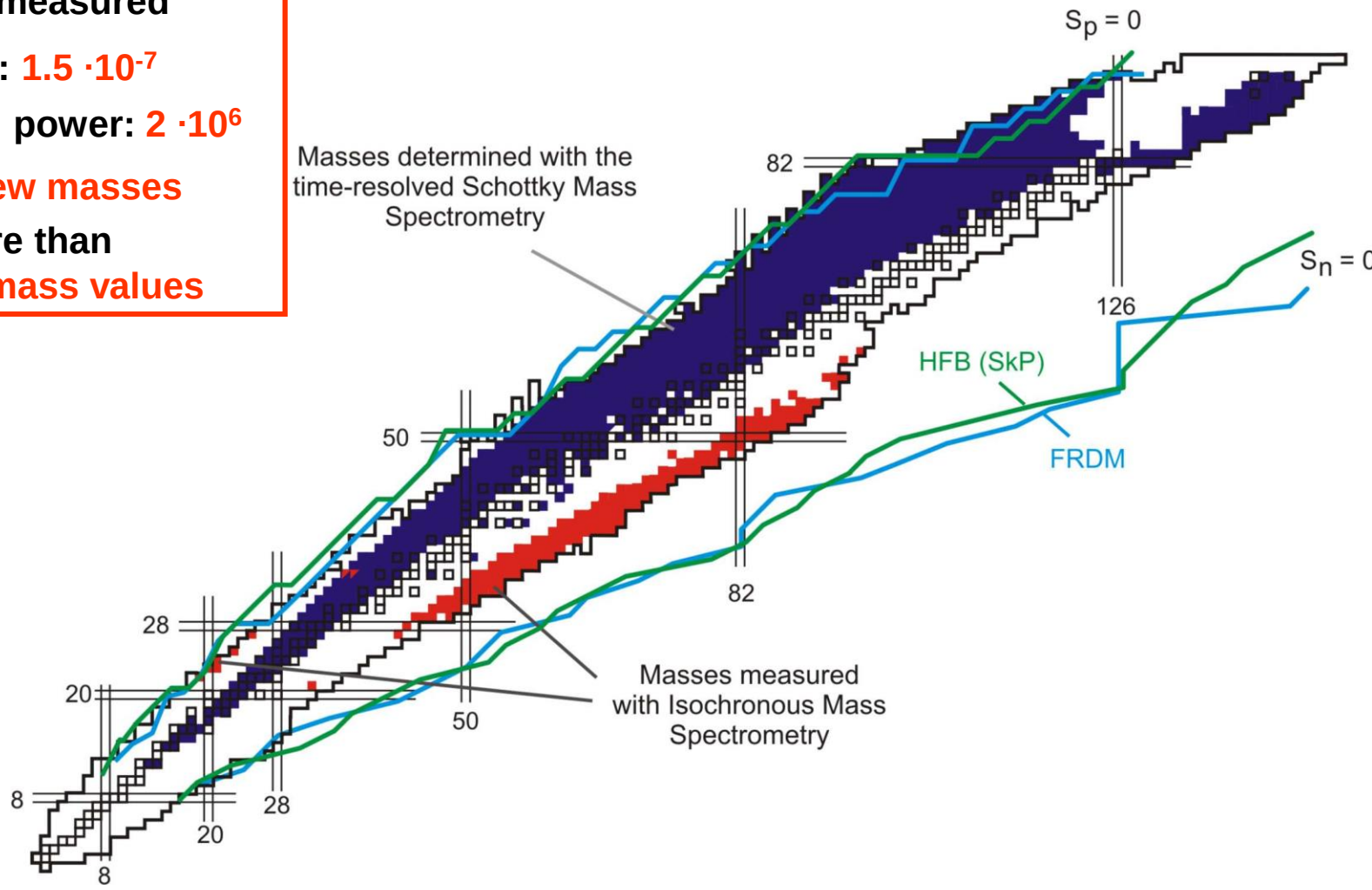

Mass Measurements of Stored Exotic Nuclei at Relativistic Energies

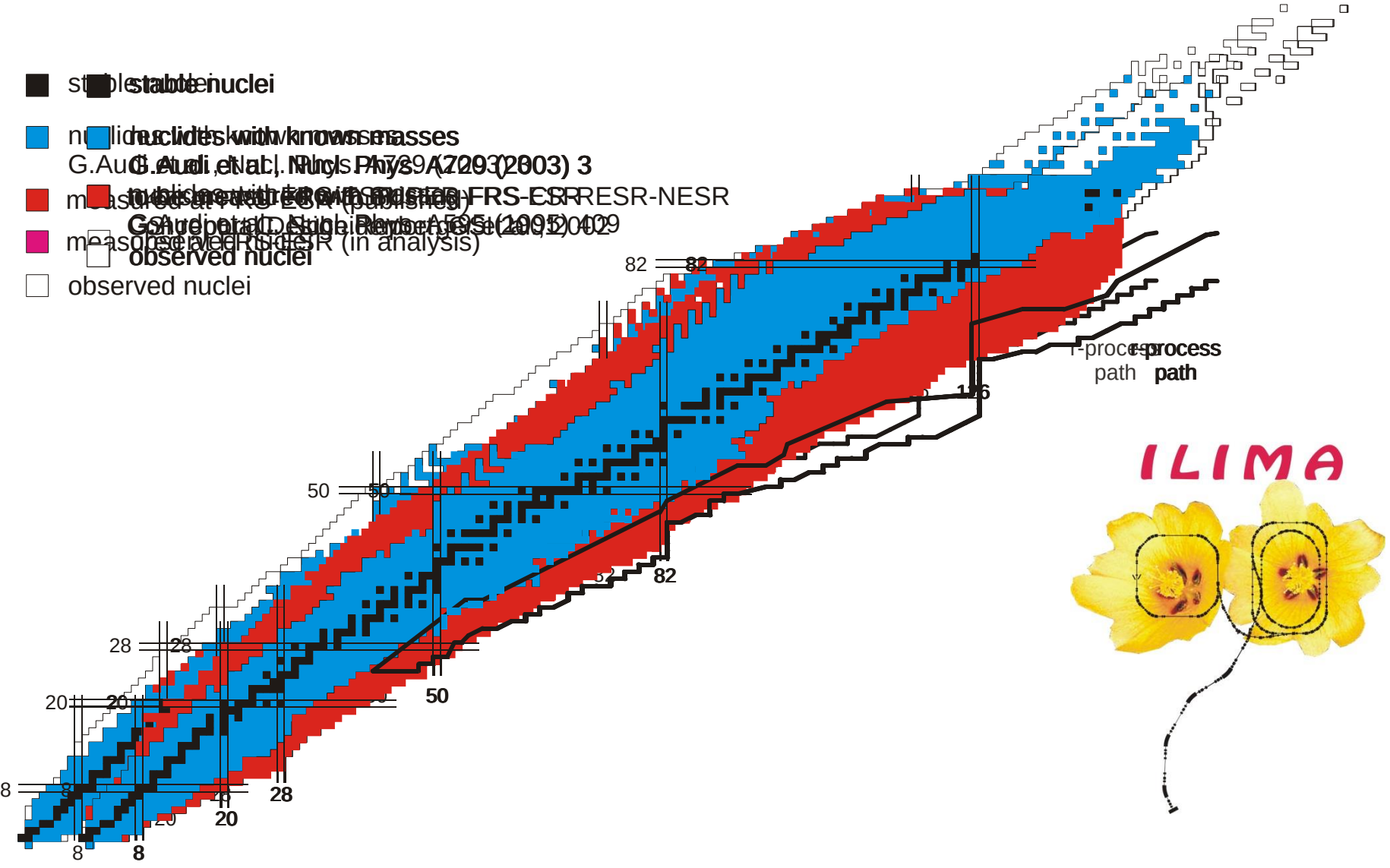

ILIMA

II. Multiple-Reflection Time-of-Flight Mass Spectrometer

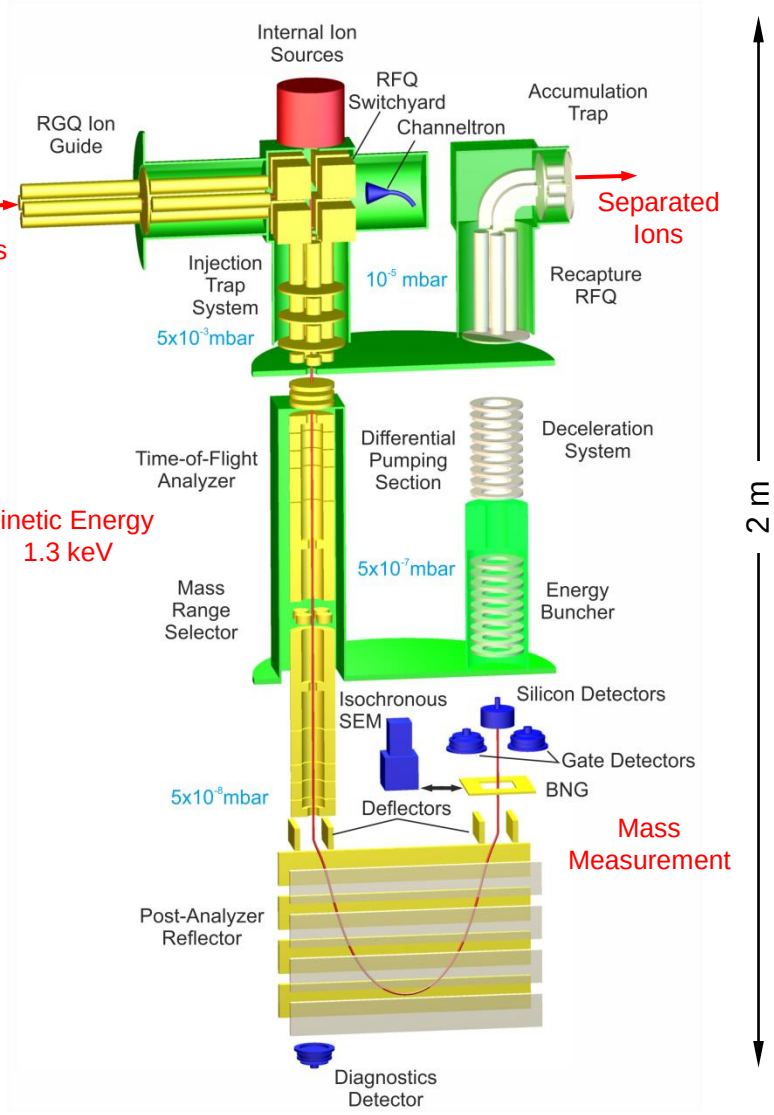

T. Dickel, W.R. Plass

Mass Resolving Power

600,000

Mass Measurement Accuracy

down to 10^{-7}

Measurement Duration

2…20 ms

Ions required for mass measurement

~ 10 ions

W.R. Plaß et al., NIM B 266 (2008) 4560
W.R. Plaß et al., Int. J. Mass Spectrom. 394 (2013) 134
T. Dickel et al., NIM A 777 (2015) 172

Full Mass Range, $m/\Delta m \sim 10^3$-10^4 | $m/\Delta m \sim 10^5$-10^6, Mass Accuracy ~ 10^{-6}-10^{-7} | $m/\Delta m > 10^5$

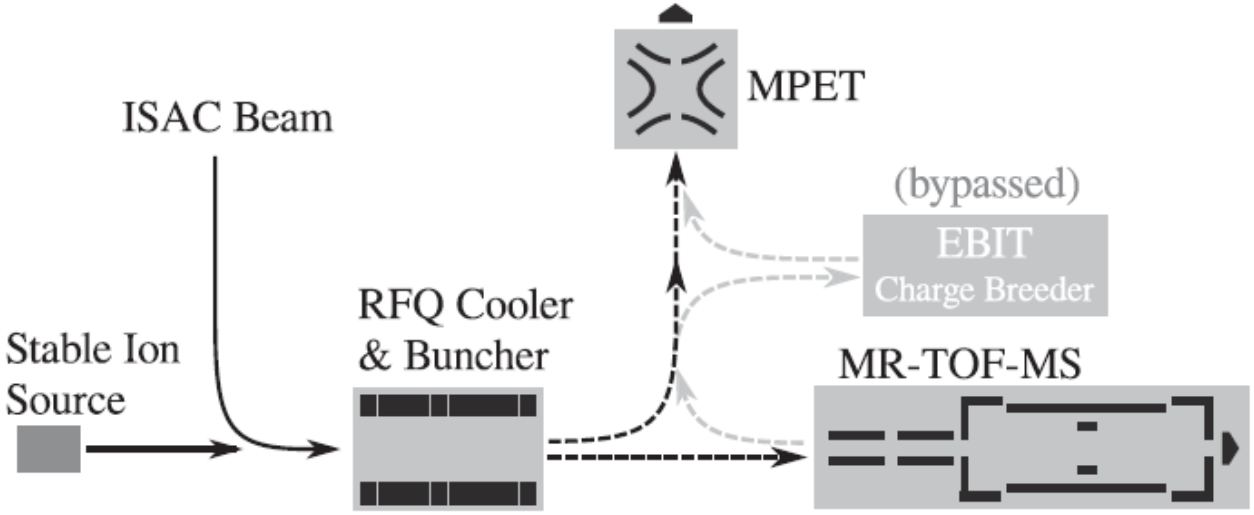

FIG. 1. Overview of the TITAN facility highlighting the main components relevant for this experiment. Beam transport of continuous beam is depicted by solid lines and transport of bunched beam is depicted by dashed lines. Transport options not used in this experiment are depicted in light gray.

E. Leistenschneider et al., „Dawning of the N = 32 Shell Closure Seen through Precision Mass Measurements of Neutron-Rich Titanium Isotopes" , Phys. Rev. Lett. 120, 062503 (2018)

(9 Feb. 2018)

TABLE I. Reported mass measurements performed during this TITAN experimental campaign with the two independent spectrometers: MR-TOF-MS and MPET, and the final TITAN combined values. All MPET mass values are referenced to the mass of ^{39}K, while references to MR-TOF-MS masses are indicated in the table. Atomic masses are presented as mass excess (ME) in keV/c^2.

Species	$ME_{MR\text{-}TOF\text{-}MS}$	ME_{MPET}	ME_{TITAN}
^{51}V	(calibrant)	−52 203.5 (1.8)	−52 203.5 (1.8)
^{51}Ti	−49 722 (15)	−49 731.5 (2.1)	−49 731.3 (2.1)
^{52}Cr	(calibrant)	−55 421.3 (2.0)	−55 421.3 (2.0)
^{52}Ti	−49 466 (16)	−49 479.1 (3.0)	−49 478.7 (3.0)
^{53}Cr	(calibrant)	−55 288.4 (1.9)	−55 288.4 (1.9)
^{53}Ti	−46 877 (18)	−46 881.4 (2.9)	−46 881.3 (2.9)
^{54}Cr	(calibrant)	−56 929.3 (4.6)	−56 929.3 (4.6)
^{54}Ti	−45 744 (16)	...	−45 744 (16)
^{55}Cr	(calibrant)	...	...
^{55}Ti	−41 832 (29)	...	−41 832 (29)

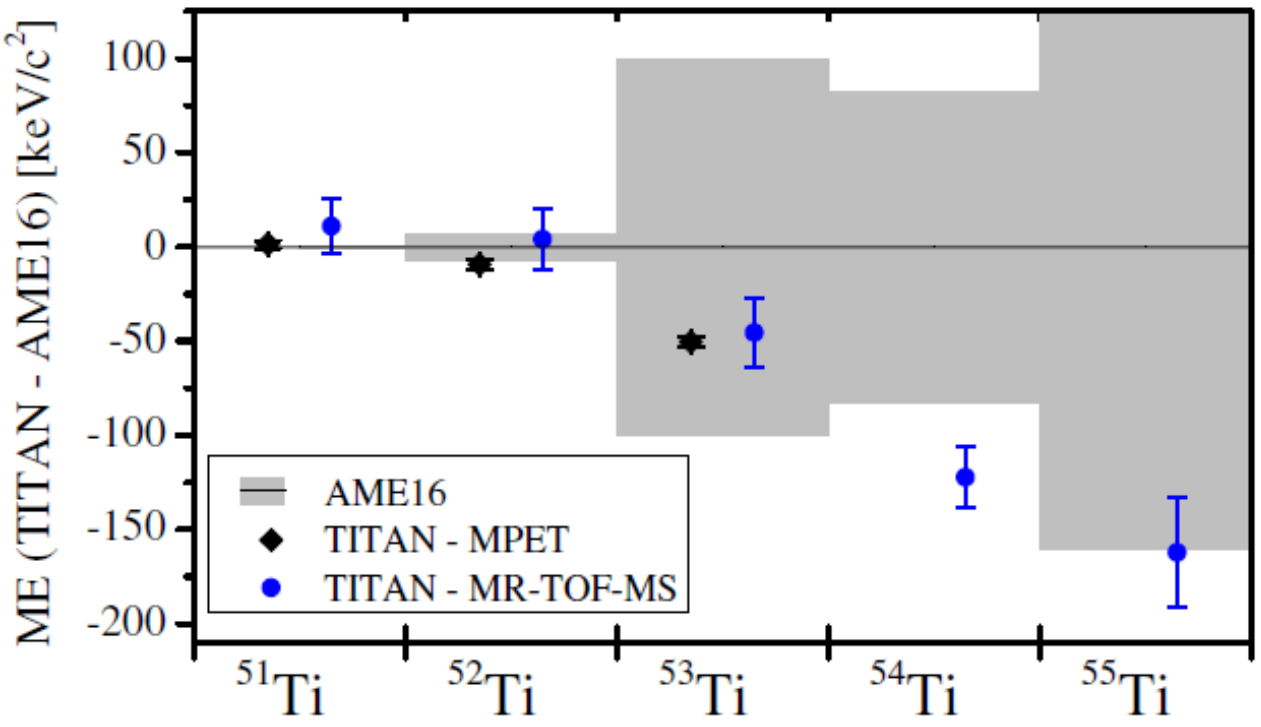

FIG. 3. The agreement between MPET and MR-TOF-MS mass measurements can be seen through their mass excesses, plotted here against the AME16 recommended values for comparison. Grey bands represent AME16 uncertainties.

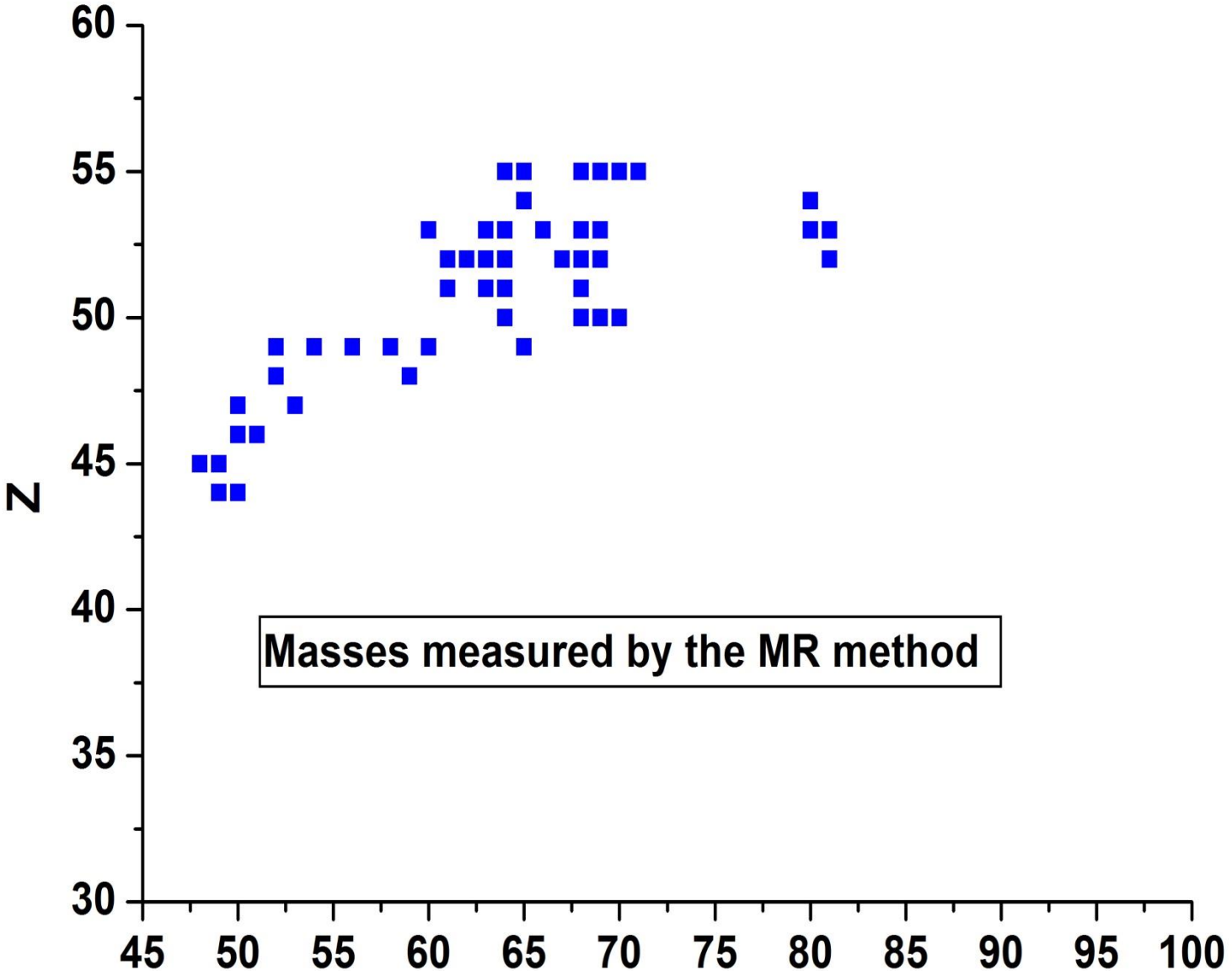
Z
60
55
50
45
40
35
30
45
50
55
60
65
70
75
80
85
90
95
100
Masses measured by the MR method

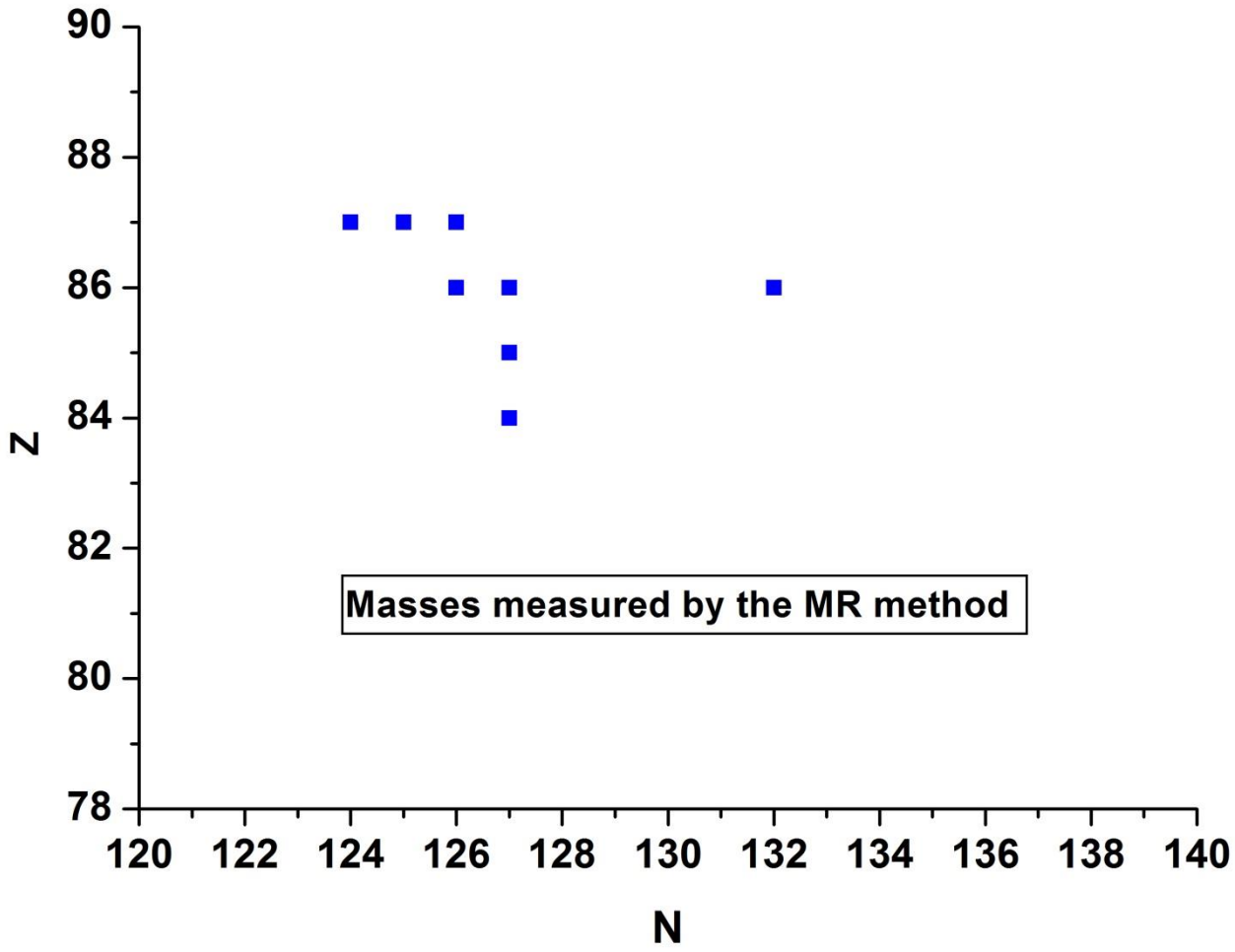
90
88
86
84
82
80
78
Z
120
122
124
126
128
130
132
134
136
138
140
N
Masses measured by the MR method

Detector tests with the prototype of the CSC for the Super-FRS and direct mass measurements of neutron-deficient nuclides below ^{100}Sn

W. R. Plaß[1,2] (Spokesperson), **T. Dickel[1,2]** (Co-Spokesperson), S. Ayet San Andrés[1,2], S. Bagchi[1,2,3], S. Beck[1,2], T. Eronen[4], H. Geissel[1,2], F. Greiner[1], E. Haettner[2], C. Hornung[1], A. Jokinen[4], A. Kankainen[4], B. Kindler[2], D. Kostyleva[1,2], N. Kuzminchuk[2], B. Lommel[2], I. Mardor[5,6], I. Miskun[1], I. D. Moore[4], I. Mukha[2], Z. Patyk[7], S. Pietri[2], A. Prochazka[2], S. Purushothaman[2], C. Rappold[1,2], S. Rinta-Antila[4], T. Saito[2,7,8], C. Scheidenberger[1,2] (GSI Contact Person), Y. Tanaka[1,2], H. Weick[2], J. Winfield[2], J.

*Regarding the proposal S474 "Detector tests with the prototype of the CSC …" the G-PAC recommends attributing **21 main shifts** to this proposal with **highest priority (A)**.*

We are looking forward to a successful experimental run and hope that you will continue to propose experiments to future calls for proposals.

Sincerely yours,

Prof. Dr. Paolo Giubellino
Scientific Managing Director

Reaction studies with the FRS Ion Catcher:

A novel approach and universal method for the production, identification of and experiments with unstable isotopes produced in multi-nucleon transfer reactions with stable and unstable beams

Regarding the proposal "Reaction studies with the FRS Ion Catcher: A novel approach and universal method for the production, identification of and experiments with unstable isotopes produced in multi-nucleon transfer reactions with stable and unstable beams" (Proposal S475), the G-PAC considers the proposal of high scientific interest.

However, due to the limited available beam time, the proposal has been placed on a reserve list ***(Category A-)****. Should it be possible to run the experiment, a total of* ***12 main shifts*** *may be used.*

Sincerely yours,

Prof. Dr. Paolo Giubellino
Scientific Managing Director

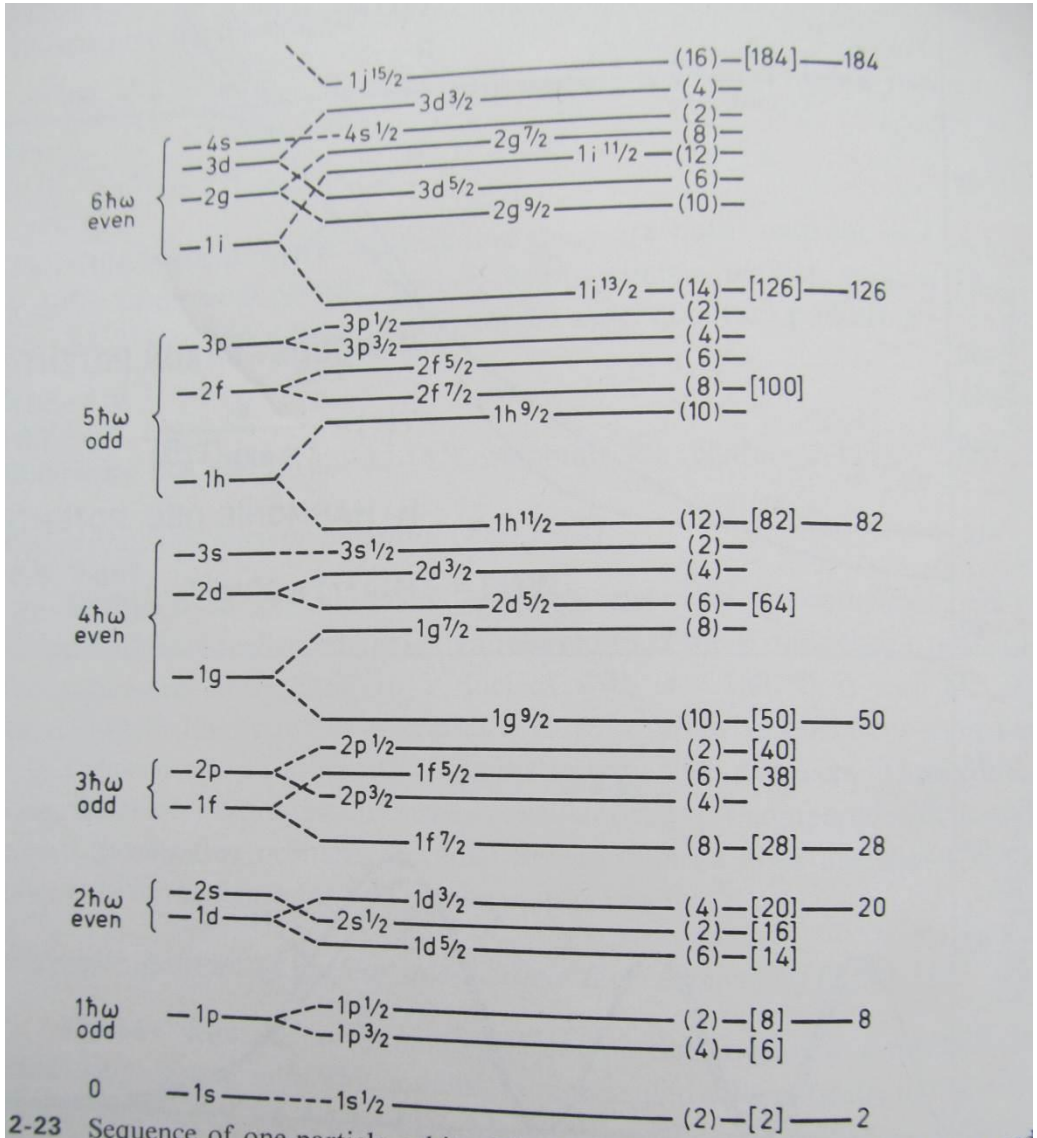

2-23 Sequence of one-particle orbits. The figure is taken from M. G. Mayer and . Jensen, *Elementary Theory of Nuclear Shell Structure*, p. 58, Wiley, New York, 1955.

pectra of odd-A nuclei compared with predictions of one-particle model
Fig. 2-24)

Single particle spectra with indicated the magic nambers for spherical nuclei. Bohr and Mottelson, Vol. I.

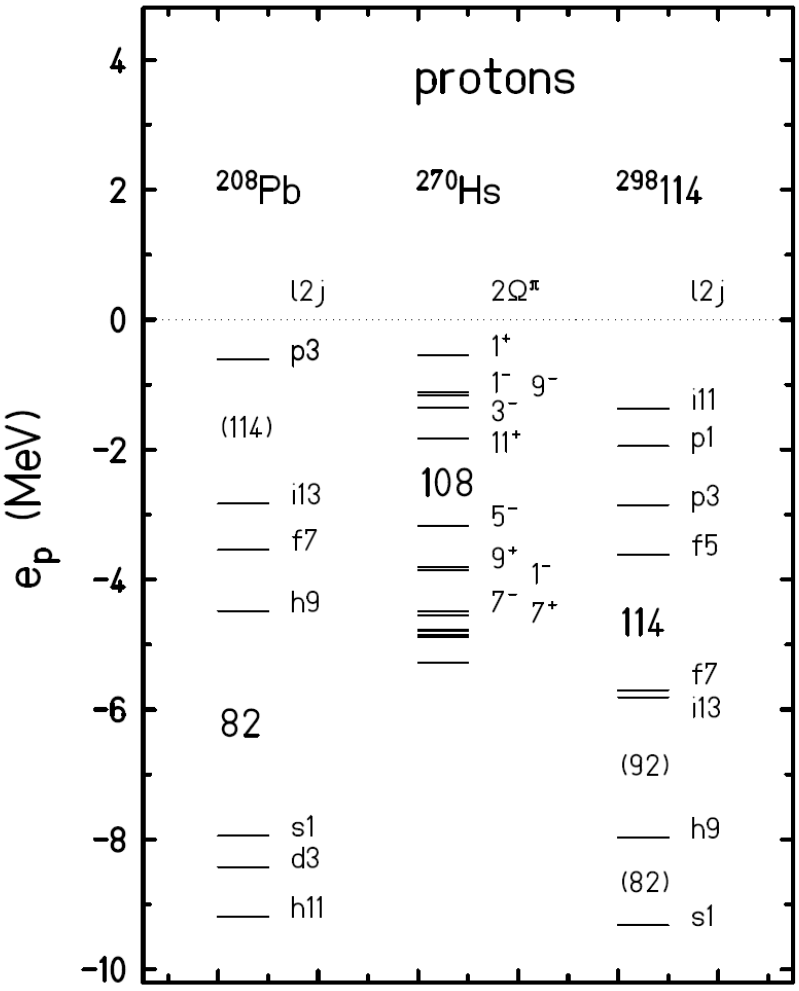

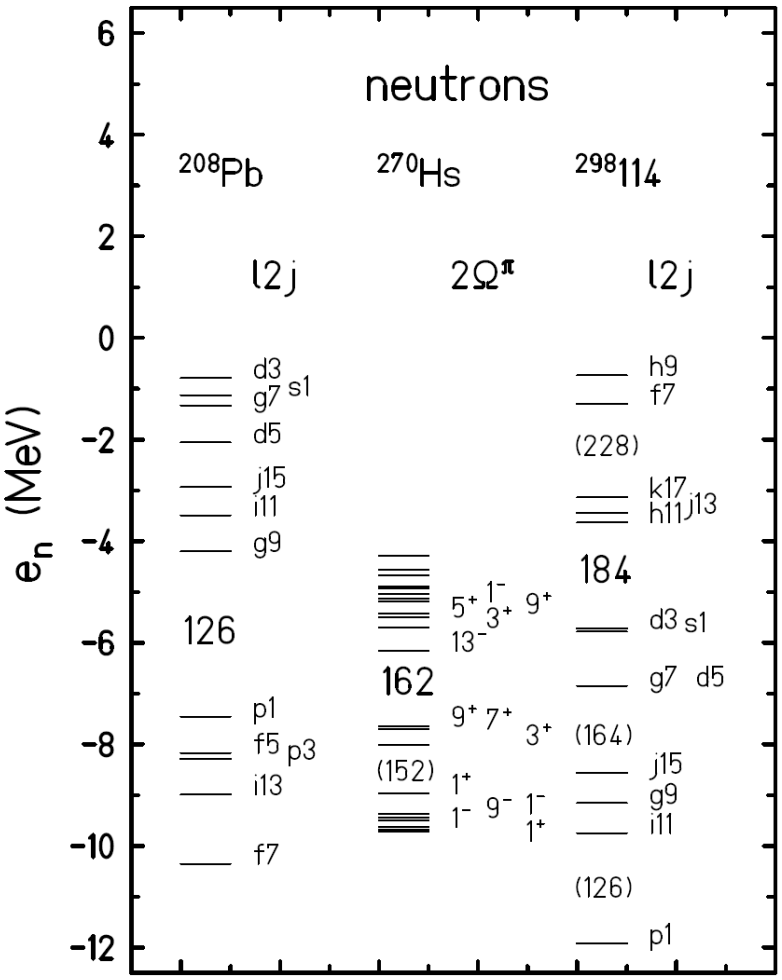

Proton and neutron single-particleWoods-Saxon energy levels calculated for three doubly magic nuclei: ^{208}Pb, ^{270}Hs and ^{298}114. Spectroscopic symbol for the orbital angular momentum *l* and the total spin (multiplied by two) 2*j* are given at each level of the spherical nuclei ^{208}Pb and ^{298}114. Projection of spin on the symmetry axis of a nucleus (multiplied by two) 2Ω and parity π are shown at each level of the deformed nucleus ^{270}Hs.

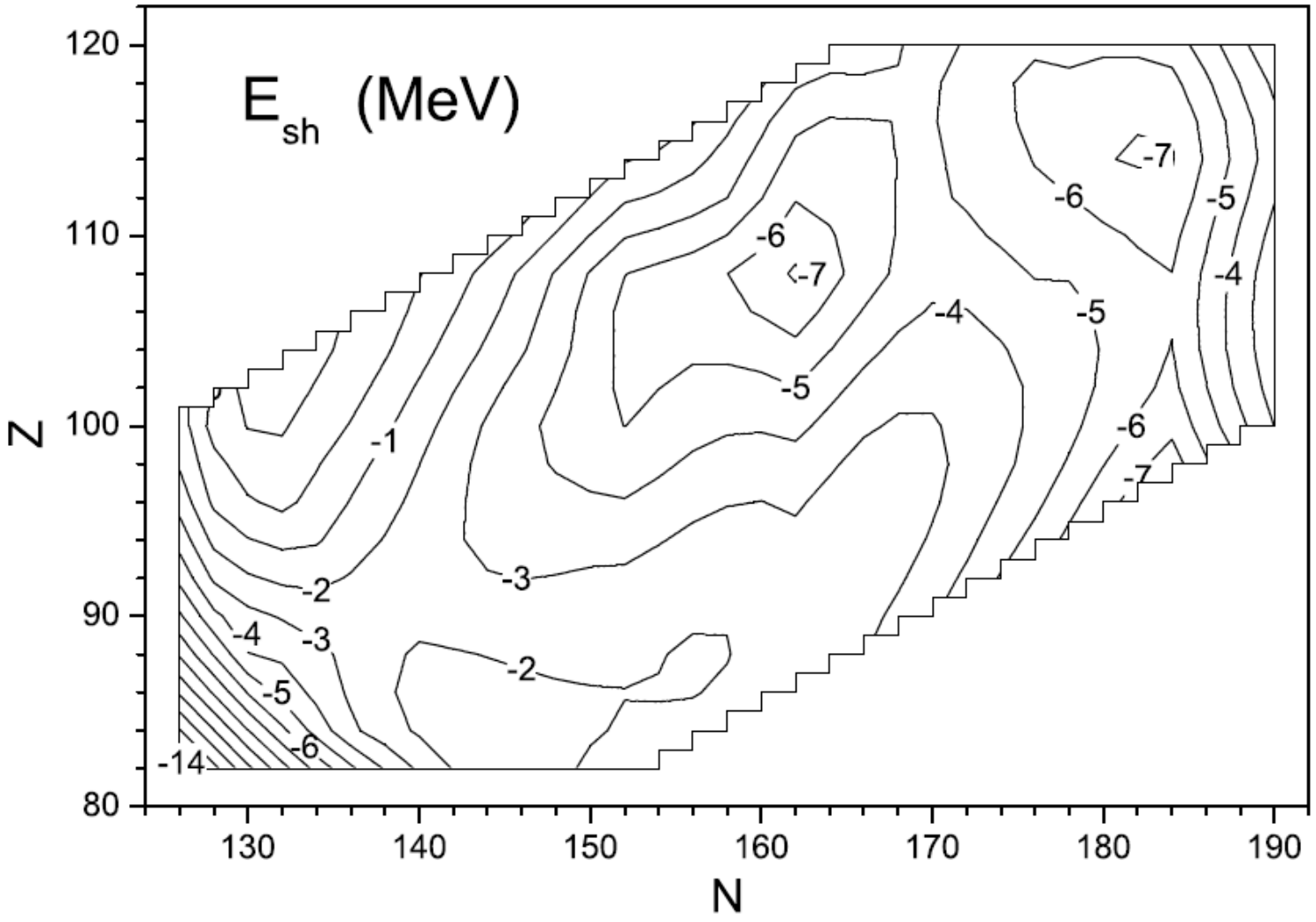

The shell correction has three minima in this region. The first one (about -14 MeV) is btained for a doubly magic spherical nucleus 208Pb. The second one (about -7 MeV)

Proprties of superheavy nuclei calculated in the macroscopic-microscopic approach.

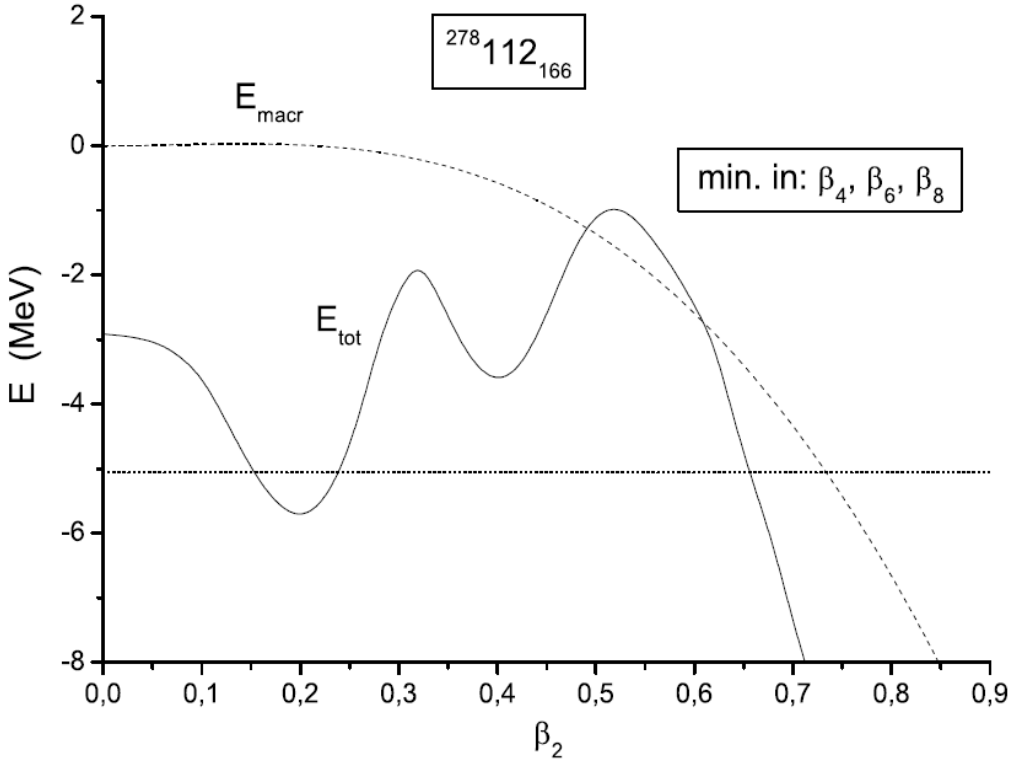

Figure 14: Spontaneous-fission barrier for the nucleus $^{278}112$.

Figure 14 gives an example of the static spontaneous-fission barrier, calculated for the deformed superheavy nucleus $^{278}112$. For so heavy nucleus, 4-dimensional space $\{\beta_\lambda\}$ λ= 2, 4, 6, 8, is sufficient for the analysis. There is no macroscopic barrier for such a heavy nucleus and that the whole barrier is created by shell effects. One can also see that the barrier is very thin. At the deformation β_2=0.66, the nucleus is already outside of the barrier.

Liquid Drop Model of Nuclear Binding Energy

The binding energy (B) per nucleon is approximately the same for all (stable) nuclei (first noticed in the early 1930s).
This led Weizsaecker in 1935 to the comparison of the nucleus with a liquid drop, which also has a constant density, independent of the number of molecules.

$$M_{atom}c^2=N*M_nc^2+Z*M_pc^2-B_N+Z*M_ec^2-B_e$$

B_{LD} (MeV) =		B/A(Pb)
+15.74063 **A**	**volume**	**15.7**
-17.61628 $A^{2/3}$	**surface**	**-3.0**
-23.42742 $(N-Z)^2/A$	**symmetry**	**-1.0**
- 0.71544 $Z^2/A^{1/3}$	**Coulomb**	**-3.9**
-12.59898 $(mod(N,2)+mod(Z,2)-1)/A^{1/2}$	**pairing**	

B/A(Pb)=7.8 MeV

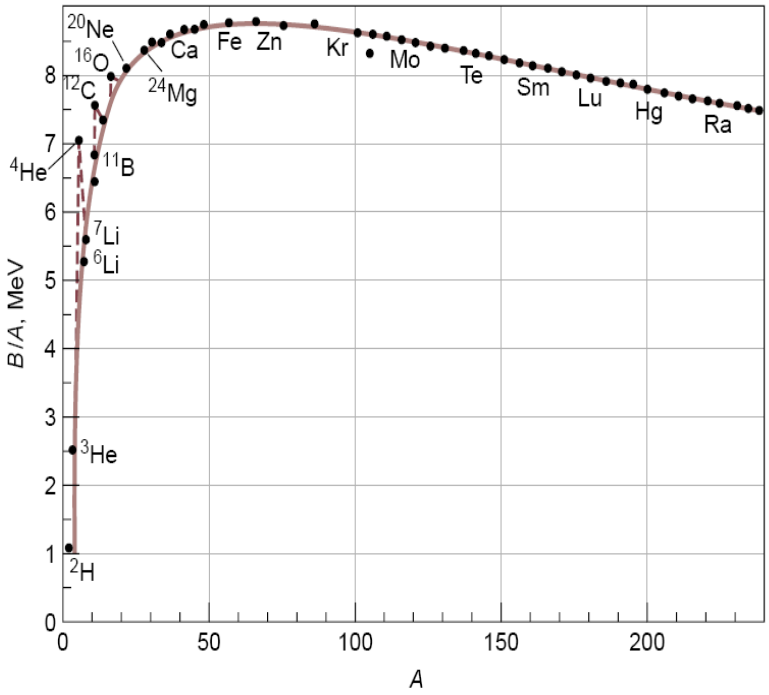

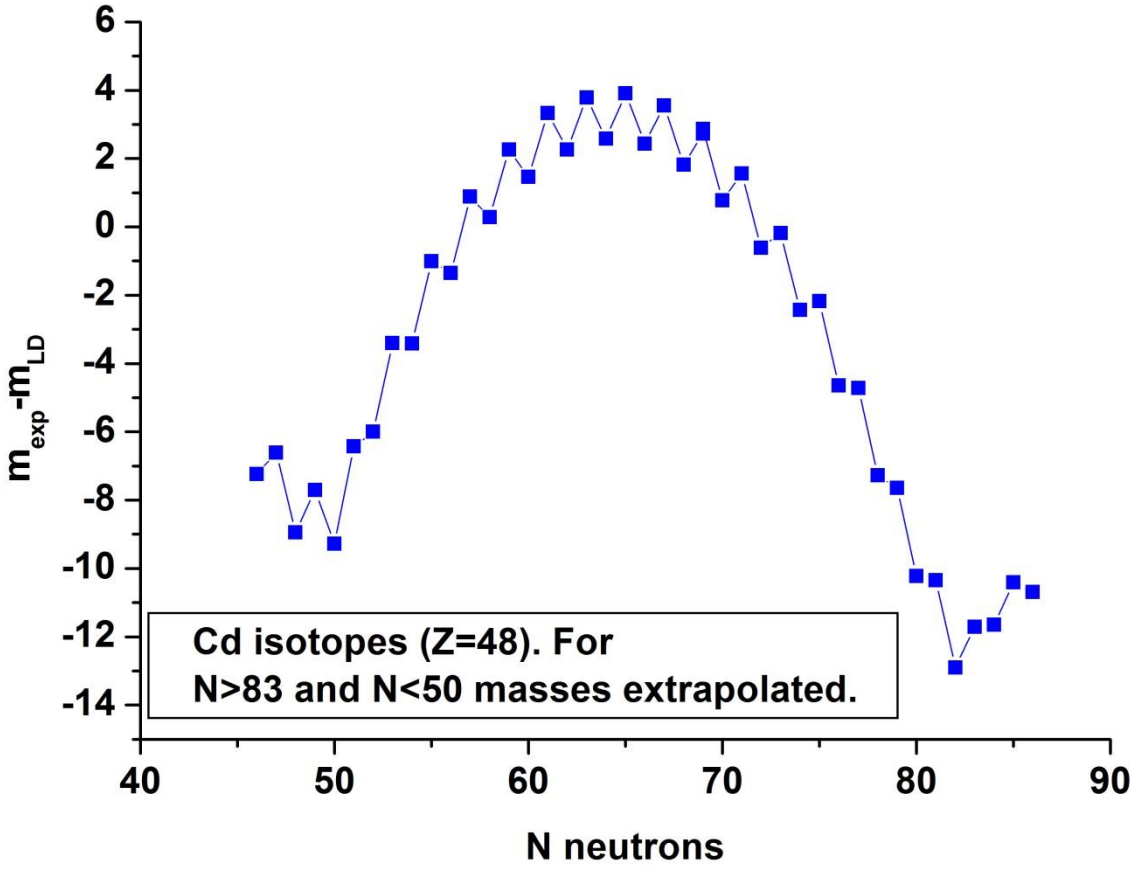
6
4
2
0
-2
-4
-6
-8
-10
-12
-14
m_{exp}-m_{LD}
40
50
60
70
80
90
N neutrons
Cd isotopes (Z=48). For
N>83 and N<50 masses extrapolated.

Exp. Shell correction extracted from measured masses AME-2016.
For an ilustration N=48. For Z=28 no shell closure.

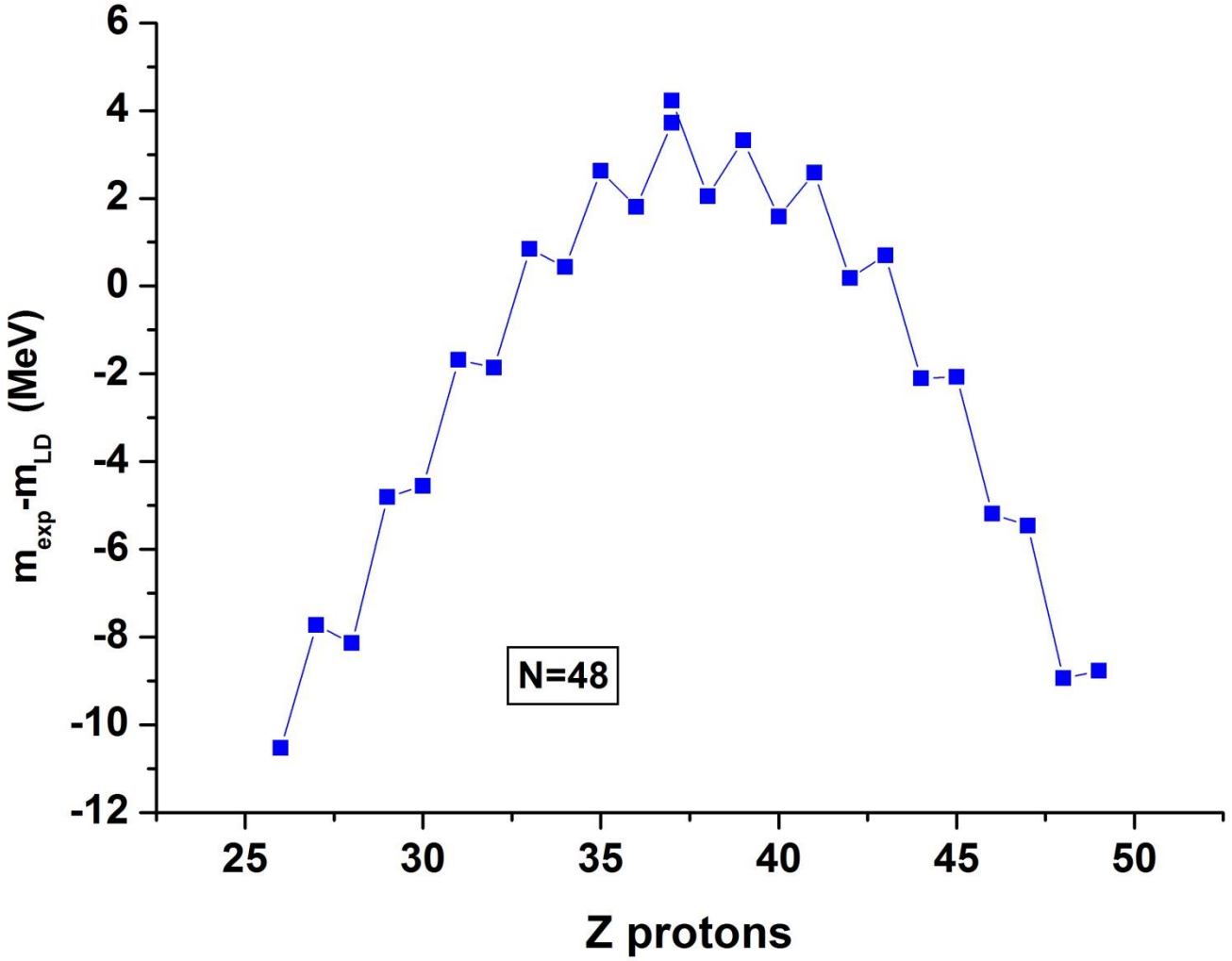

Comparison with Theory

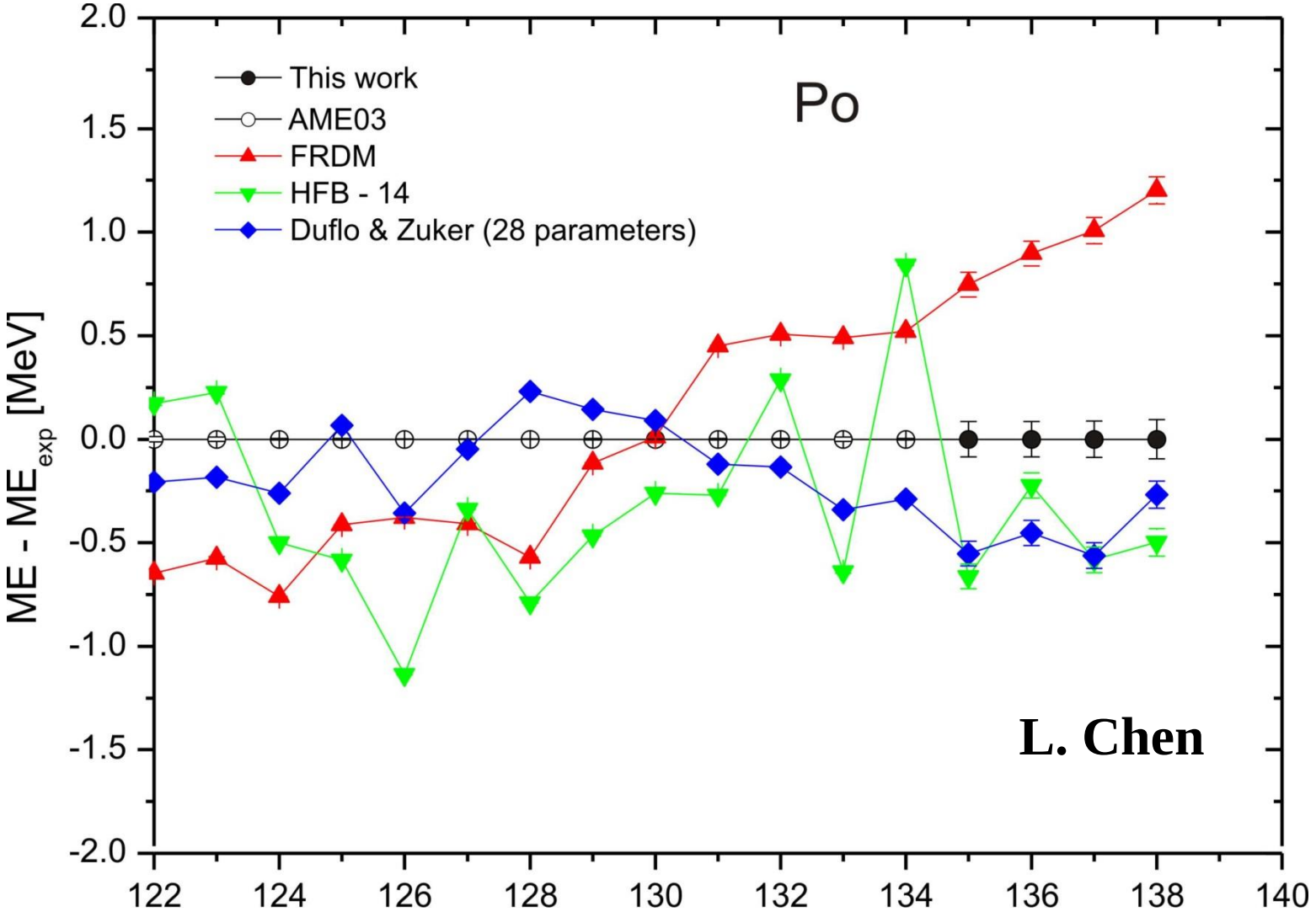

Detailed illustration of the accuracy of currently used nuclear-mass models

A. Sobiczewski [a,b,c,*], Yu.A. Litvinov [c], M. Palczewski [a]

Atomic Data and Nuclear Data Tables 119 (2018) 1–32

The rms and average value, $\bar{\delta}$, of the discrepancies calculated for the global ($Z, N \geq 8$), light ($8 \leq Z < 28, N \geq 8$), medium-I ($28 \leq Z < 50$), medium-II ($50 \leq Z < 82$), heavy ($Z \geq 82$) and heaviest ($Z \geq 100$) nuclei, obtained with the use of the specified models, are given. The numbers of nuclei with masses both calculated and evaluated in 2012, N_{nucl}, are also shown.

Model	LSD	FRDM	FRDM12	TF	HFB21	GHFB	DZ	KTUY	INM	WS3+	WS4+	HN
Year	2003	1995	2016	1996	2010	2009	1995	2005	2012	2010	2014	2001
No.	1	2	3	4	5	6	7	8	9	10	11	12
Global												
N_{nucl}	2316	2353	2353	2351	2353	2353	2353	2353	2353	2353	2353	
rms	0.608	0.654	0.579	0.649	0.572	0.789	0.394	0.701	0.362	0.248	0.170	
$\bar{\delta}$	−0.027	−0.059	−0.010	0.027	0.030	−0.103	−0.032	−0.058	−0.011	−0.008	0.000	

indicated with N_{nucl}. The N_{nucl} values provide information on how many masses are involved in the corresponding comparison. The accuracy is expressed by the rms (root-mean-square) values of the discrepancies between the calculated and experimental masses:

$$\mathrm{rms}^2 = \frac{1}{N_{\mathrm{nucl}}} \sum_{i=1}^{N_{\mathrm{nucl}}} (m_{\mathrm{th}} - m_{\mathrm{exp}})^2.$$

Also given are the average values of the discrepancies:

$$\bar{\delta} = \frac{1}{N_{\mathrm{nucl}}} \sum_{i=1}^{N_{\mathrm{nucl}}} (m_{\mathrm{th}} - m_{\mathrm{exp}}).$$

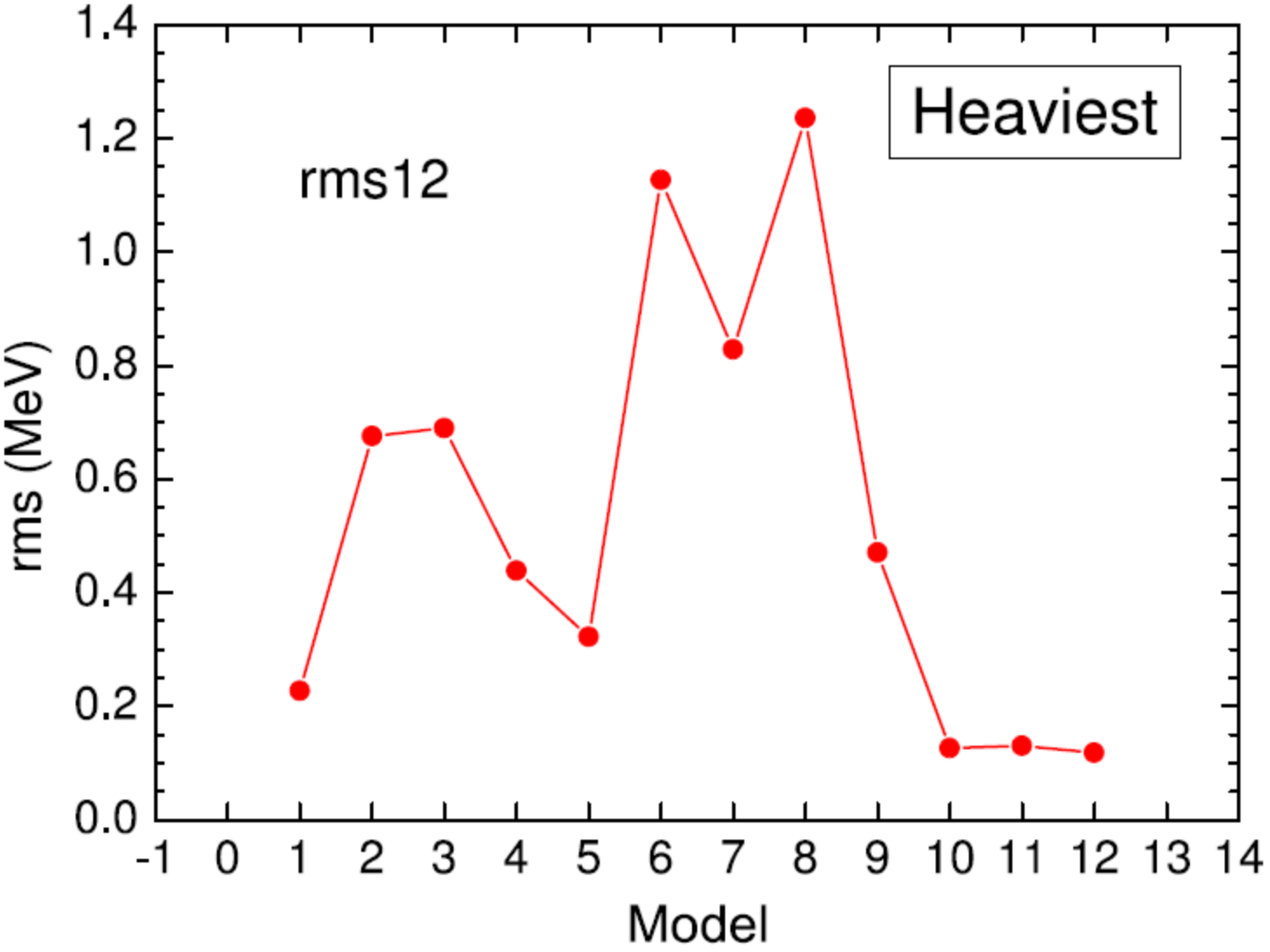

Fig. 5. (Color online) Same as in Fig. 3, but in the region of the heaviest nuclei.

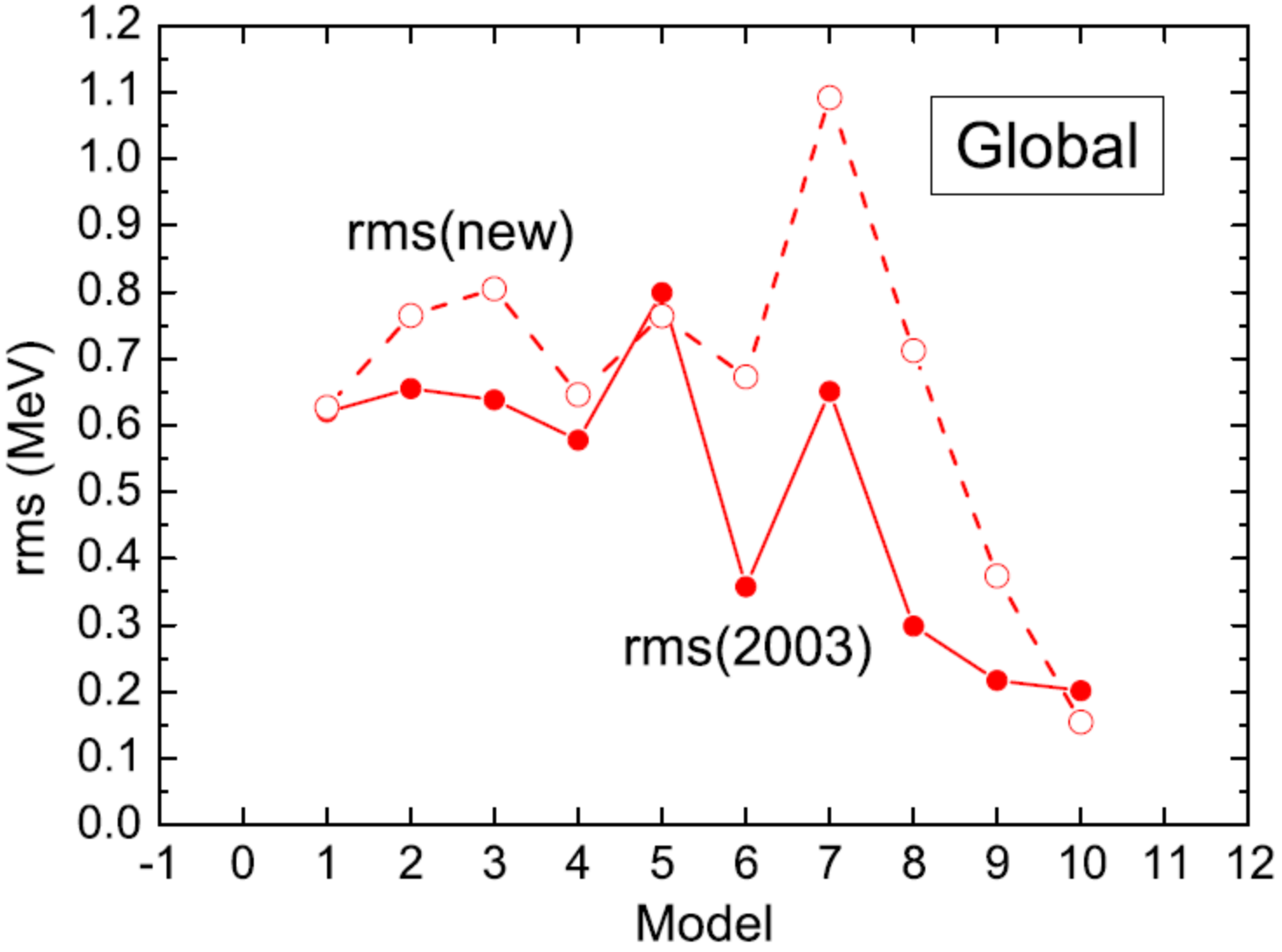

Fig. 6. (Color online) The dependence of the rms(2003) and rms(new) discrepancies on the model for the global region of nuclei. Each model is identified by the number (from 1 to 10) prescribed to it in Table B.

Streszczenie

- **W GSI Darmstadt wyznaczono ponad 300 mas jąder atomowych metodą SMS lub IMS.**
- **Czas chłodzenia elektronami w metodzie SMS jest rzędu 1 s.**
- **Metodą IMS można mierzyć masy jąder o czasie życie rzędu 1 ms, ale błąd pomiaru jest dosyć duży >100 keV.**
- **Metodą MR-TOF-MS wyznaczono wartości mas dla izotopów Ti z dokładnością <20 keV dla nuklidów żyjących dłużej niż 490 ms.**
- **Modele teoretyczne opisują zmierzone masy z dokładnością ok. 500 keV**